ELSEVIER

Surface functionalization of SBA-15 by the solvent-free method

Yi Meng Wang, Zheng Ying Wu, Jian Hua Zhu*

Mesoscopic Laboratory, Department of Chemistry, Nanjing University, 22 Hankou Road, Nanjing City, Jiangsu Province 210093, China

Abstract

A solvent-free technique was employed for fast modification of mesoporous materials. Copper, chromium and iron oxide species could be highly dispersed in SBA-15 by manually grinding the corresponding precursor salts and the host, followed by calcinations for the first time. This method is more effective to spontaneously disperse oxide species onto SBA-15 than impregnation, probably forming monolayer or submonolayer dispersion of salts or oxides. Besides, Cr(VI) species dominate in the mixing sample while Cr(III) species dominate in the impregnation one. In the temperature programmed surface reaction of nitrosamines, the sample prepared by solvent-free method showed a higher catalytic activity than the impregnation one.
© 2004 Elsevier Inc. All rights reserved.

1. Introduction

Appearance of order mesoporous materials affords a new type of candidate for catalysts and adsorbents, because their large pore size enables the active centers to be accessible for the large feedstock molecules. Despite numerous research works being focused on the mesoporous materials, it is still difficult for them to replace the common microporous catalysts based on zeolite, and one of the reasons is their inherent weakness. For example, either MCM-41 or SBA-15 consist of only silica and suffer the lack of metal ion so that they lack the necessary active species for catalysis. For a similar reason, both MCM-48 and SBA-15 were inferior to zeolite in the adsorption of volatile nitrosamines [1,2]. Therefore, modification of these siliceous mesoporous materials becomes the key step to facilitate their application in industry, and numerous metals, metal oxides (sulfides), acid groups and organic functionalities have been incorporated by direct synthesis (one-pot method) or post-synthesis. The most widely employed method is impregnation with solutions of simple

thermally unstable precursor salts (e.g. nitrates, chlorides and acetates) [3,4]. In order to obtain molecularly dispersed oxide species, organic metal precursors are used to react with acidic silanol group as bases and then grafted on the surface of ordered mesoporous materials. However, this grafting method generally achieves lower loading than the former one. Moreover, organic precursor species are more complex and expensive in this procedure [4,5]. The other two less popular methods are the solid-state exchange and the loading via the gas phase by a volatile precursor and subsequent calcinations [6–8]. Although solid-state exchange has been widely studied in the synthesis of modified zeolites [9], few solid-state studies are devoted to the supported mesoporous materials. This may contribute to the absence of cationic sites in the structure of ordered mesoporous materials. Regardless of the methods used, the crucial and ultimate purpose is to achieve highly dispersed, especially molecularly dispersed, oxide species on the support, which involves the interactions and reactions of the ordered mesoporous supports and the precursors, and relates to their physical and chemical properties, as well as to the structural nature of the ordered mesoporous support [5,10].

*Corresponding author. Fax: +86-25-8331-7761.
E-mail address:* jhzhu@netra.nju.edu.cn (J.H. Zhu).

Nonetheless, most of these processes need to use solution, which not only requires extra energy to remove the solvent but also sometimes causes waste. More important, the surface of support undergoes the soakage-drying procedure, which changes not only the surface state of the host, but also the dispersion or distribution of the guest. Besides, competitive adsorption of solvent molecules will disturb the guest–host interaction, which may hinder the dispersion and anchoring of the active component species. To seek solvent-free modification of mesoporous materials, we try to disperse oxide species on the SBA-15 and MCM-41 highly by finely mixing the supports and metal precursor salts along with the subsequent calcinations. This method will exploit the reactivity of the rich surface silanol groups of mesoporous support, using nitrate or acetate to suppress the tendency of metal to agglomerate into metal oxide domains and providing an effective means to disperse oxide species finely. However, there were some suspicions on the solid-state method in the regime of ordered mesoporous materials. Schüth et al. claimed that the wet impregnation sample has smaller hematite particles and higher activity in the oxidation of SO_2 to SO_3 than the solid-state impregnation sample [3]. On the contrary, Mou and coworkers found that physically mixed samples have lower rates of deactivation and higher catalytic activities than solution impregnation ones in both fresh and regenerated tubular MCM-41-supported MoO_3 catalysts for ethylbenzene dehydrogenation reaction [6]. These opposite evaluations prompt us to investigate the solvent-free method in this article, dispersing copper, chromium and iron oxide species on SBA-15 or MCM-41, and our aim is to disperse metal oxide species on SBA-15 through the spontaneous dispersion of salts or oxides. Furthermore, the substantially different dispersion capacities of SBA-15 and MCM-41 supports provide us a chance to understand the nature of this solvent-free method.

2. Experimental

2.1. Sample preparation

Tetraethylorthosilicate (TEOS) was supplied by factory and used here as the silica source. Amphiphilic triblock copolymer poly(ethylene oxide)-poly(propylene oxide)-poly(ethylene oxide) $EO_{20}PO_{70}EO_{20}$ (Pluronic P123) was purchased from Aldrich. Other regents were used as received without any purification.

SBA-15 silicas were synthesized in a similar way as those originally reported by Zhao et al.[11] using P123 as the template. In a typical synthesis, 4.0 g of P123 copolymer was dissolved in 150 g of 1.6 M HCl, followed by addition of 8.50 g TEOS at 313 K. The resulting mixture was stirred for 24 h and then placed in

an oven at 373 K for 24 h under static condition. Silica products were filtered, washed and dried. Pure silica MCM-41 was synthesized following the standard method using the C_{16} surfactant [12]. Silica gel with 60–80 meshes is a commercial product from the Qingdao Haiyang Chemical Factory.

The templates of all the ordered mesoporous materials were removed by calcination at 823 K for 6 h in air before the physical mixing or impregnation. For the solvent-free method, the template-free SBA-15 and the precursor salts were manually ground together in the mortar at room temperature to achieve a homogeneous mixture and then heated to 773 K at a rate of 2 K/min, held at this temperature for 6 h. In different cases, the precursor salts were $Cu(NO_3)_2 \cdot 3H_2O$, $Cr(NO_3)_3 \cdot 9H_2O$ and $Fe(NO_3)_3 \cdot 9H_2O$, respectively, and the obtained samples were denoted as mixMO_x/SBA-15(X), where MO_x and X represent metal oxide species and the MO_x mass percentage in the composites, respectively. To help with the interpretation of results, a few additional samples have been prepared ad hoc: silica gel or the template-free MCM-41 are physically mixed with the precursors and then calcined, as described above. For preparation of the traditional impregnation samples, the template-free SBA-15 was immersed in a minimum amount of salt solution at the required concentration and then dried at 373 K, finally calcined at 773 K for 6 h. The samples were denoted as impMO_x/SBA-15(X), where MO_x and X have the same meaning as those in mixMO_x/SBA-15(X).

2.2. Characterization

The materials were characterized by powder X-ray diffraction recorded on an ARL XTRA diffractometer with Cu$K\alpha$ radiation in the 2θ ranges from 0.5 to 8° or from 5 to 70°. IR experiments were performed on a set of BRUKER 22 FT-IR spectrometer, and the UV–Vis diffuse reflectance (DR) spectra were recorded on a UV-2401 (Shimadzu) spectrophotometer adapted with a praying mantis accessory using $BaSO_4$ as standard. UV–Vis-NIR diffuse reflectance spectroscopy was carried out on Perkin-Elmer Lambda 900 spectrometer, the data were written directly to a computer disk at 2 nm intervals as percent reflectance relative to the Spectralon® standard. XPS measurements on the VG ESCA-Lab MKα instrument were performed using a 1253.6 eV $K\alpha$ magnesium X-ray source, the energy scale of spectrometer was calibrated by setting the measured C1S binding energy to 284.6 eV. The concentration of each element was then calculated from the area of the corresponding peak, calibrated by using the relative sensitivity factor of Wagner.

In the temperature programmed surface reaction (TPSR) test, a 20-mg sample was activated in N_2 at 773 K for 2 h except for the mixCuO/SBA-15(5) sample

calcined at 573 K, that sample was activated at 573 K in order to not change the chemical environment of copper species on SBA-15. N-nitrosopyrrolidine (NPYR, Sigma) solution was injected in the sample at 313 K, followed by purge of N_2 for 0.3 h [1]. The cracking products of nitrosamines were detected every 20 K by the spectrophotometric method [2].

3. Results and discussion

3.1. Dispersion of metal oxides on SBA-15

Figs. 1 and 2 illustrate the XRD patterns of SBA-15 samples modified through the solvent-free method and impregnation. It is clear that the former method can disperse copper and chromium oxide species on the support much better. For mixCuO/SBA-15 samples, the dispersion threshold was up to 15 wt%, much higher than that of impCuO/SBA-15 sample, but less than 5 wt%, as shown in Fig. 1A. For comparison, the template-free MCM-41 and silica gel were chosen as the control support to be mixed with cupric nitrate

(A)

(B)

Fig. 2. The wide angle XRD patterns of (a) mixCrO$_x$/SBA-15(NO$_3^-$), (b) mixCrO$_x$/SBA-15(Cl$^-$) and (c) impCrO$_x$/SBA-15(NO$_3^-$) with Si/ Cr = 11.4, and (d) mixFeO$_x$/SBA-15, (e) impFeO$_x$/SBA-15 with Si/ Fe = 5.
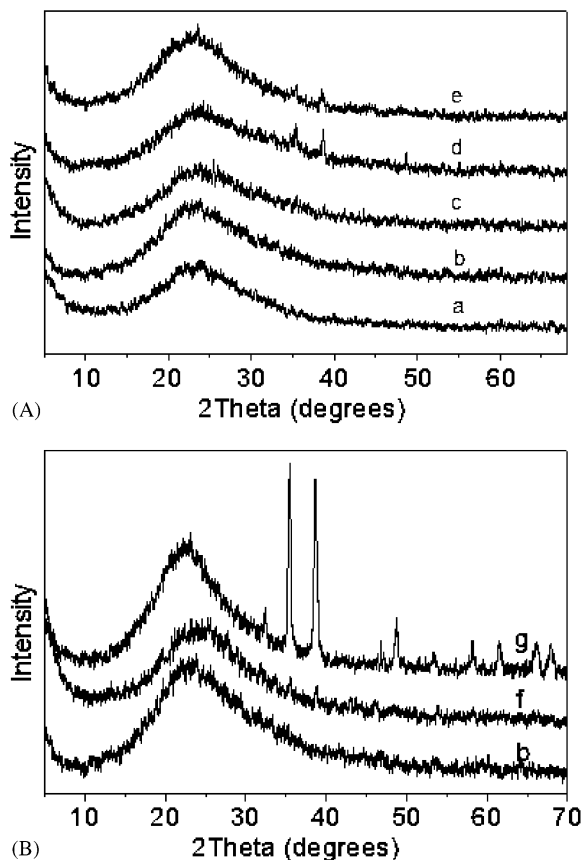

(A)

(B)

Fig. 1. The wide angle XRD patterns of (a) mixCuO/SBA-15(5), (b) mixCuO/SBA-15(10), (c) mixCuO/SBA-15(15), (d) mixCuO/SBA-15(20) and (e) impCuO/SBA-15(5), (f) mixCuO/MCM-41(10) and (g) mixCuO/SiO$_2$(10).
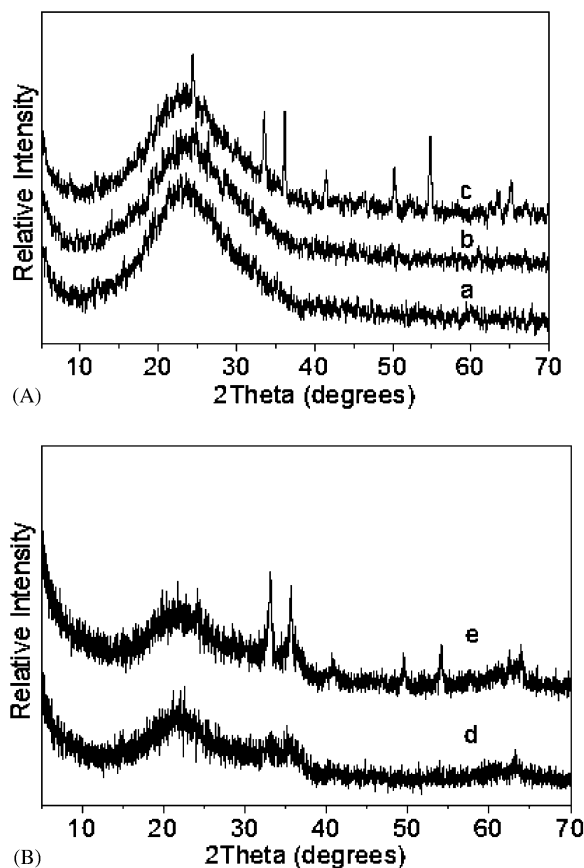
trihydrate, but the crystalline CuO phase did appear in both samples with a 10 wt% loading of CuO, although the CuO reflection intensities on the MCM-41 sample were much weaker than those on the SiO$_2$ sample (Fig. 1B). SBA-15 and MCM-41 have comparable surface areas 953 and 990 m^2/g, respectively. SBA-15 is an analogue of MCM-41 with larger pores, thicker pore walls and superior hydrothermal stability, but SBA-15 has a somewhat less condensed silica framework than MCM-41 [11], and the distinct feature that renders SBA-15 different from MCM-41 is the presence of connections between parallel mesopores [13] and rich surface silanol groups. On the other hand, the commercial silica gel showed a rather small surface area of 410 m^2/g and a < 5% weight loss in the calcinations at 1073 K for 2 h, meaning rather less silanol groups on the surface to condensate and thus exhibiting the worst dispersion of copper oxide as mentioned above. Hence, it seems reasonable to relate the high dispersion of copper guest on SBA-15 to the rich surface silanol groups and probably unique dual pore structure of the host.

A further proof on the advantage of the solvent-free method came from the chromium-modified SBA-15 with

a Si/Cr molar ratio of 11.4; the peaks of crystalline Cr_2O_3 clearly appeared on the XRD patterns of impregnation sample but were absent on the mixed sample (Fig. 2A). For FeO_x/SBA-15 samples with a Si/Fe ratio of 12, no difference was observed on the XRD patterns of both mixed and impregnation samples (figure not shown). In order to compare with the results of FeO_x/MCM-41 reported by Schüth et al.[3], FeO_x/SBA-15 samples with a Si/Fe ratio of 5 were prepared by the solvent-free method and the incipient wetness impregnation, and calcined following the same procedure in the literature [3]. However, impFeO$_x$/SBA-15 (Si/Fe = 5) clearly showed the sharp reflections characteristic for larger hematite particles, while only glabrate ones appeared in the case of mixFeO$_x$/SBA-15 (Si/Fe = 5), as seen in Fig. 2B. This result is quite different from that of MCM-41, where mixed sample (Si/Fe = 5) gave rise to the sharp reflections. Since a content of 1 wt% is sufficient to cause sharp peaks in the XRD pattern for crystalline transition metal compounds [14], the XRD results of mixed samples indicate a well-spontaneous dispersion of oxides guest on SBA-15, proving the efficiency of the solvent-free method to prepare MO_x/SBA-15 composites.

Introduction of copper oxide in SBA-15 made the intensities of reflections (100), (110) and (200) all decayed, as observed on the sample of mixCuO/SBA-15, due to the decreasing contrast between walls and pore space, which can be very sensitive to the distribution of matter [15,16]. After loading CuO with 10 wt%, the reflection (100) height of impCuO/SBA-15(10) reduced about 28%, while for mixCuO/SBA-15(10) this value was 16%. Surprisingly, the corresponding value of mixCuO/SBA-15(20), where the crystalline CuO phase appeared reached 25%, is still smaller than that of impCuO/SBA-15(10). No doubt the intensity decay of the reflections in impCuO/SBA-15 samples was more pronounced than that in mixCuO/SBA-15. Such behavior can be rationalized by taking into consideration that the Cu introduced may have different impact on the reflection intensities depending on its ordering or distribution: if the copper forms a monolayer on the internal walls, it contributes to the spatial order giving rise to the diffraction pattern itself [17]. If disordered, however, it represents a pore-filling medium of higher electron density than air and therefore causes strong intensity losses. Hence, the overall intensity loss in mixCuO/SBA-15 will be smaller than that of impCuO/SBA-15, because on the latter sample copper was disorderly deposited and the crystalline CuO phase appeared earlier with a 5 wt% loading. Based on all these results, it can be concluded that CuO species can spontaneously disperse onto the surface of SBA-15, probably forming a monolayer in this solvent-free process.
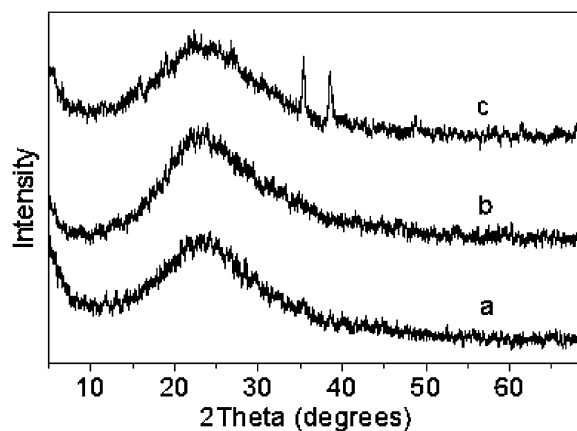

Fig. 3. Wide angle XRD patterns of the mixCuO/SBA-15(10) sample prepared from different precursor salts: (a) acetate, (b) nitrate and (c) chloride.

Figs. 2 and 3 show the influence of anion on the dispersion of oxide on SBA-15. Crystalline CuO and Cr_2O_3 phases emerged when the hydrated chlorides replaced the corresponding hydrated nitrates with the same loading amount, but cupric acetate hydrate did have such effect. In liquid–solid or gas–solid systems, the precursor is anchored to the hydroxyl groups of the support by a hydrogen-bonding or a ligand exchange mechanism [7,8], where anions bridged the hydroxyls of support and the cation of precursor salts. In solid–solid systems, anions mediate the interaction between the surface hydroxyl of support and cations in the precursor. Both nitrate and acetate anions have a π-system electronic structure and act as bidentate ligands to form hydrogen bonds with the silanols easily, while chlorides interact with the surface silanol groups relatively weak. Hence, nitrate and acetate favor the formation of Si–O–M over the formation of M–O–M during the heating, while chloride has a tendency to condensate to metal oxide clusters.

3.2. Characterization of modified SBA-15 composites

Fig. 4A plots the XPS spectra of CuO/SBA-15(5) samples, in which two $Cu2p_{3/2}$ peaks can be distinguished on the mixCuO/SBA-15(5) calcined at 773 K: one at 932.8 eV and the other at 935.8 eV, associated with the CuO (933.74 eV) and Cu–O–Si–O– (936.14 eV) species [18]. In case of impCuO/SBA-15(5), the $Cu2p_{3/2}$ peak mostly lay at 932.8 eV, and the surface content of CuO that was calculated from XPS data was only 3.16% by weight, deviating much from the content in the sample (5 wt%), while the data in mixCuO/SBA-15 was 5.53% by weight, quite close to the content of 5 wt%. XPS is well known as a surface-sensitive technique; oxide or salt dispersed on the support as monolayer will give an XPS signal much stronger than that given by the corresponding mixture of oxide or salt with the support,
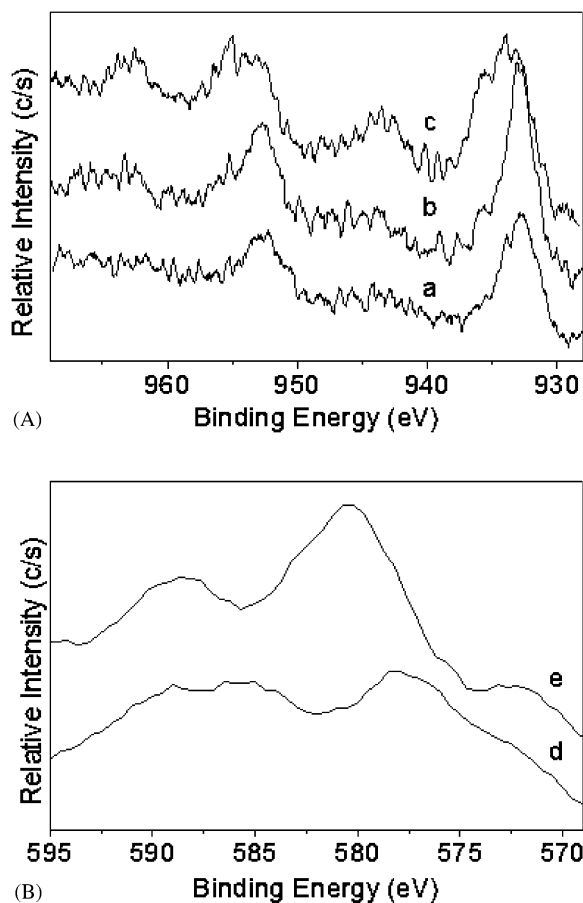
Fig. 4. XPS spectra of (a) impCuO/SBA-15(5) calcined at 773 K, (b) mixCuO/SBA-15(5) calcined at 573 K and (c) 773 K, (d) impCrO$_x$/SBA-15, and (e) mixCrO$_x$/SBA-15 with the same molar ratio Si/Cr = 11.4.

and this predication has been borne out well by the XPS studies on MoO$_3$/TiO$_2$, MoO$_3$/γ-Al$_2$O$_3$, MoO$_3$/SiO$_2$, WO$_3$/γ-Al$_2$O$_3$, WO$_3$/SiO$_2$, ZnO/SiO$_2$, and CuCl//γ-Al$_2$O$_3$ [14]. Hence, the XPS data indicate a high dispersion of copper oxide species on the SBA-15 by the solvent-free method, while the oxides aggregated in the impregnation samples, in good agreement with the XRD results. In addition, the intensity ratio of the satellite peak to the corresponding principal peak of Cu2$p_{3/2}$ (I_{sat}/I_{pp}) was found to be about 0.27 for impCuO/SBA-15(5) but 0.36 for mixCuO/SBA-15. The increasing I_{sat}/I_{pp} values reveal that the dispersed CuO$_x$ species change their coordination environment [18].

Fig. 4B shows two distinct Cr2$p_{3/2}$ peaks in the samples of mixCrO$_x$/SBA-15(10) and impCrO$_x$/SBA-15(10), an ∼580.4 eV peak for Cr(VI) dominated in the former while a ∼578.0 eV peak dominated mainly for Cr(III) in the latter. It is the first time to find that the preparation method can determine the oxidation state of active oxide species on the support, say, Cr(VI) dominates in the mixed sample while Cr(III) is predominant in the impregnation sample. The dominat-

ing Cr(VI) species in the mixed sample may be due to a higher dispersion, leading to a fast oxidation during the calcination. Furthermore, the surface Cr/Si molar ratio in the former is 0.073, higher than 0.067 in the latter and closer to the bulk chromium content (0.087), which proves that the solvent-free method enables CrO$_x$ species equably dispersed onto the surface of SBA-15 [19].

The different oxidation state of chromium species on SBA-15 can be also approved by the color and UV DR spectra of CrO$_x$/SBA-15 samples. The calcined impregnation samples were green ascribed to Cr$_2$O$_3$ species, far from the orange–red color in the mixed sample that came from CrO$_3$ species. Besides, the sample of impCrO$_x$/SBA-15(10) clearly showed a strong d–d band at ∼595 nm along with two shoulders near 645 and 700 nm (Fig. 5A), indicating that Cr^{3+} is the main species, though the existence of few Cr^{6+} species cannot be excluded. In the case of mixCrO$_x$/SBA-15 (10), absence of these d–d bands along with the strong
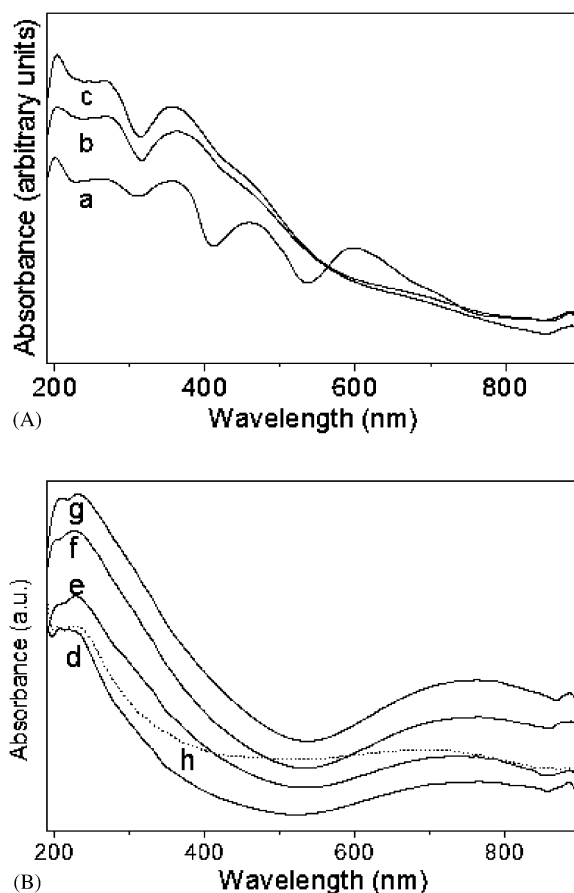

Fig. 5. UV DR spectra of (a) impCrO$_x$/SBA-15 prepared from Cr(NO$_3$)$_3$·9H$_2$O, mixCrO$_x$/SBA-15 prepared from (b) Cr(NO$_3$)$_3$·9H$_2$O or (c) CrCl$_3$·6H$_2$O with the same molar ratio Si/Cr = 11.4; (d) mixCuO/SBA-15(5), (e) mixCuO/SBA-15(10), (f) mixCuO/SBA-15(15), (g) mixCuO/SBA-15(20), and (h) impCuO/SBA-15(5) (dot line).

intensities of CT transitions at 229 and 265 nm indicated the dominance of Cr^{6+} species. Since the number, wavelength and intensity of d–d bands depend on the oxidation state and coordination environment (octahedral, tetrahedral, etc.), whereas the $O \rightarrow Cr^{6+} (d^0)$ CT transitions are responsible for the intense orange color of calcined chromium oxide catalysts [20], no doubt the oxidation states of chromium species on these two samples are different, and the solvent-free method tends to disperse $Cr(VI)O_x$ species on SBA-15. Oxidation state is an important factor affecting the catalytic function of chromium-modified composites [21]. A high amount of Cr(VI) may be an indication of the high performance in the catalytic decomposition of PCDDs/PCDFs [19]. As one of the most important members in the family of commercial polyolefin catalysts, Phillips catalyst is still responsible for several million tons of commercial production of polyolefins including HDPE and LLDPE, where CrO_3 is directly impregnated onto SiO_2. Hence, the dominating Cr(VI) species in the $mixCrO_x$/SBA-15 samples predict high catalytic performance in olefin oligomerization or selective decomposition of NO_x.

Fig. 5B lists the UV DR spectra of CuO/SBA-15 samples that consist of a band above 500 nm areas due to d–d transitions of dispersed Cu^{2+} species ($3d^9$). Usually the intensity of the d–d band increased with Cu content; at the same time, the values of the maximum shifted toward lower wavelength, meaning an increased nuclearity of the oxidic clusters (CuO_x species) [18]. Nonetheless, when the CuO loading of mixCuO/SBA-15 sample reached 20 wt%, the d–d band did not shift to a lower wavelength substantially, indicative of less CuO_x clusters, if any, on these samples. In contrary, the impCuO/SBA-15(5) showed a d–d band with the maximum at 714 nm, much lower than 780 nm for the mixCuO/SBA-15(5) sample, mirroring the existence of CuO_x clusters on the impregnation sample detectable in XRD patterns. Hence, UV data further prove the high dispersion of CuO on SBA-15 by this solvent-free method.

All these results confirm that the solvent-free method is an efficient way to highly disperse oxide species on the ordered mesoporous materials such as SBA-15, which is paramount for the preparation of catalyst because most heterogeneous catalysts need nanometer-sized particles to be dispersed on a high-surface-area support. The efficiency of this method may arise from the strong interactions between the precursor nitrates or the final oxide species and the supports during the whole mixing–heating process, relate to the spontaneous monolayer dispersion of the guest on supports [14]. The surface bond between the monolayer of the guest and the surface of the host is strong enough to make the entropy effect a determinative factor for $\Delta G < 0$, resulting in the widespread occurrence of monolayer or submonolayer dispersion [14]. As mentioned above in

the XPS test, the appearance of higher $Cu2p_{3/2}$ (935.8 eV) or $Cr2p_{3/2}$ (578.0 eV) binding energy on the samples prepared by the solvent-free method is a forceful proof to confirm the existence of such surface bond.

Since the interaction of oxide species with the SBA-15 surface is expected to consume silanol groups, careful analysis of the IR transmission spectra of the two CuO/SBA-15(10) samples was carried out. The surface silanol groups ($\equiv$Si-OH) stretching modes give rise to bands in the region 960–990 cm^{-1} of the IR spectra of both amorphous and crystalline silicates [22–24]. The 960 cm^{-1} band in most ordered mesoporous materials indicates the presence of perturbing or defect groups, and it could be attributed to asymmetric stretching of Si–O bond neighboring surface silanol groups in CuO/SBA-15(10) samples. This band appeared near 960 cm^{-1} in the impCuO/SBA-15(10) sample, but degenerated to the shoulder of the 1080 cm^{-1} band in the mixCuO/SBA-15(10) sample (Fig. 6), which means that more surface silanol groups are consumed in the mixing–heating process in comparison with wet impregnation. That is to say, the surface silanol groups interacted with the guest species and can be depleted in the solvent-free method; although some silanol groups contacted with the solvent during the impregnation process, they can be recovered after drying the sample. Pretreatment at high temperature suppresses the surface silanol group of the support. In case of $mixFeO_x$/SBA-15 (Si/Fe = 5) sample, the $\sim$960 cm^{-1} band gradually weakened with the heating temperature increasing (Fig. 7). However, an open question remains for the IR spectra of $mixCrO_x$/SBA-15 (Si/Cr = 11.4), since this band was well reserved but maximized at a lower frequency of $\sim$948 cm^{-1} while an $\sim$960 cm^{-1} band still existed for the $impCrO_x$/SBA-15 (Si/Cr = 11.4) sample. A similar phenomenon occurred on the zinc modified SBA-15, where the formation of a zinc silicate monolayer on the mesopore
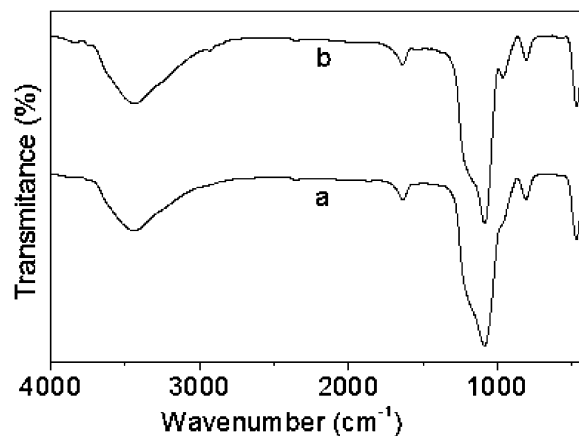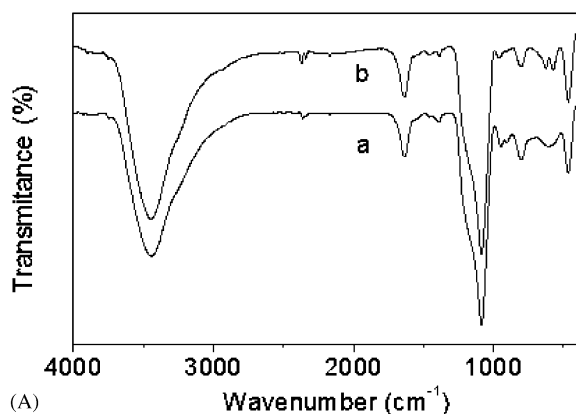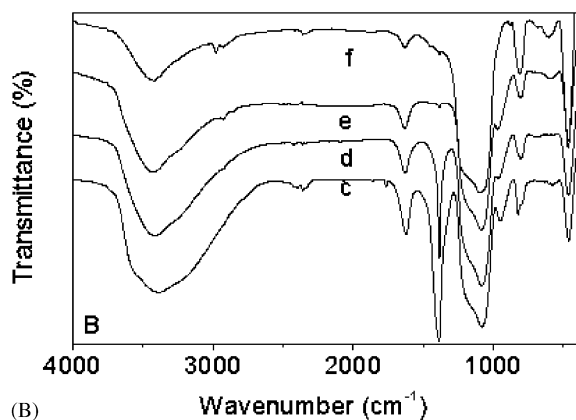

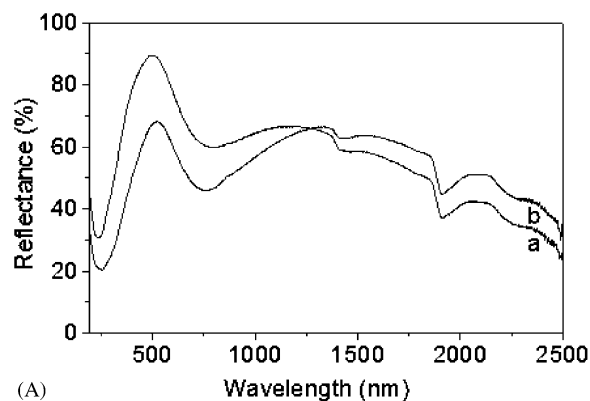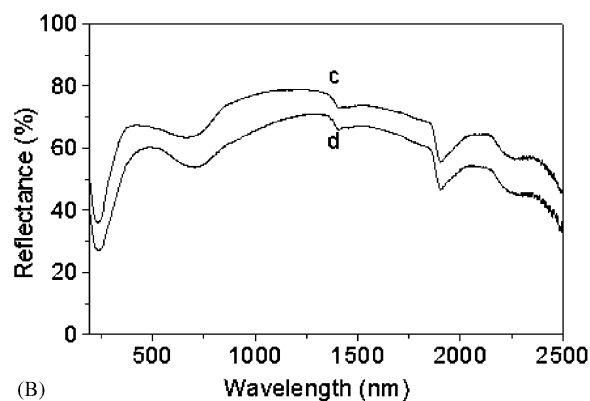Fig. 6. IR spectra of (a) mixCuO/SBA-15(10) and (b) impCuO/SBA-15(10).

(A)

(B)

Fig. 7. IR spectra of (a) mixCrO$_x$/SBA-15 (Si/Cr = 11.4), (b) impCrO$_x$/SBA-15 (Si/Cr = 11.4), and mixFeO$_x$/SBA-15 (Si/Fe = 5) pretreated at (c) room temperature, (d) 373 K, (e) 673 K, (f) 973 K.

(A)

(B)

Fig. 8. UV–Vis-NIR DR spectra of (A): (a) mixCuO/SBA-15(5), (b) mixCuO/SBA-15(10); (B): (c) impCuO/SBA-15(3), (d) impCuO/SBA-15(5).

walls was confirmed while no consumption of free groups could be detected [16]. This problem is subject to further studies.

Fig. 8 illustrates the UV–Vis-NIR DR spectra of mixCuO/SBA-15(10) samples with bands at 240 (A), 780 (B), 1410 (C) and 1910 (D) nm. Bands A and B are assigned to CT transition and d–d transition, respectively [18,25]; the other two bands C and D in the NIR region are attributed to the combination and overtone bands mainly from the surface hydroxyl groups and to a smaller extent from water [26]. With the copper loading increasing in the samples prepared by this solvent-free method (Fig. 8A), the reflectance of bands A and B decreases while that of bands C and D increases. The opposite variations of bands relating to the copper and silanol group suggested the consumption of the surface silanol groups. Conversely, the reflectance of bands A–D decreases with the copper loading increasing in the samples via impregnation, as shown in Fig. 8B. Although the disturbance of water could not be completely eliminated by carefully preheating all the samples at 373 K overnight, the different variations for these bands suggested that copper species and support

underwent different interaction during the solvent-free and the wet-impregnation process. This result further validates the high reactivity between the surface silanol groups and precursor salts in the solvent-free method.

To further investigate the role played by the surface properties of SBA-15 in this solvent-free process, the template-free SBA-15 support was further heated at 923 K for 3 h before physically mixing with Cu(NO$_3$)$_2$·3H$_2$O and Cr(NO$_3$)$_3$·9H$_2$O, since SBA-15 calcined at 923 K was still well ordered, but the surface properties were greatly altered by prominent dehydroxylation [13]. Using this support in the solvent-free method, the crystalline CuO phases obviously appeared by XRD analysis when the CuO loading reached 10 wt%, and sharp CuO peaks presented in the sample of a 15 wt% CuO. In case of chromium, with the same loading of Si/Cr = 11.4, peaks of crystalline Cr$_2$O$_3$ phase emerged. Also, the color of this sample turned to green mottled and some brown, quite different from the orange–red of the corresponding sample prepared with SBA-15 calcined at 823 K, but similar to the green of the impregnation sample. Correlating the difference between the dispersion capacity of SBA-15 and MCM-41 to the different condensation degrees between these two mesoporous materials and along with the above results,

it can be concluded that high dispersion of copper oxide species onto SBA-15 owes to the rich-surface silanol groups. The loss of dispersion ability of the support preheated at 923 K should not be ascribed to the disappearance of interconnectivities between the main mesopores, because of the retention of these complementary pores up to 1173 K [13]. The role of the secondary porosity bridges in SBA-15 cannot be validated or excluded yet at present, so, the rich surface silanol groups of support play the key role in this solvent-free method.

3.3. Catalytic behavior of the modified SBA-15 composites

Copper-incorporated SBA-15 prepared by wet impregnation exhibited a high efficiency in trapping volatile nitrosamines despite the pore size of SBA-15 being tremendously larger than the molecular diameter of volatile nitrosamines [27]. Therefore, NPYR, one of the volatile nitrosamines, was used as the probe to survey the catalytic function of copper-incorporated SBA-15 for degradation of nitrosamines. To prevent protonation impact of the catalyst [2], the reaction is carried out in nitrogen instead of hydrogen atmosphere and the amount of NO_x released represents the decomposed nitrosamines. For the sample of mixCuO/SBA-15(5), the total amount of NO_x formed in the whole process (39.7 μmol/g) was more than that of the impCuO/SBA-15(5) (33.7 μmol/g). Besides, the amount of NO_x released by the former sample increased rather slowly, with a maximum at 453 K, while the amount of NO_x released by the latter sample jumped suddenly at 473 K with a maximum (Fig. 9). NPYR will decompose at a temperature higher than 573 K on the other catalysts without the introduction of copper species or other active components. Hence, the mixCuO/SBA-15(5) sample can degrade more NPYR at a relative lower temperature, mirroring the high dispersion of copper oxide species in SBA-15.
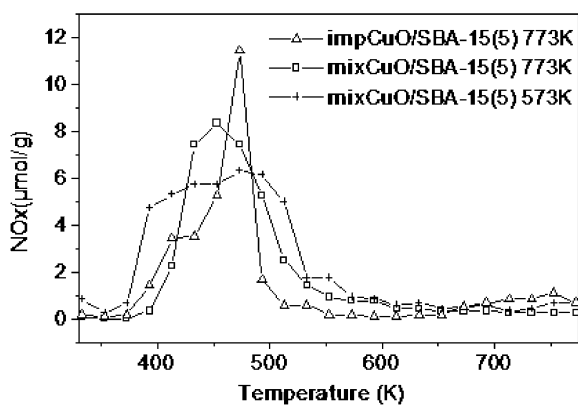

Fig. 9. Profile of NO_x released in the TPSR process of NPYR on CuO/SBA-15 samples.
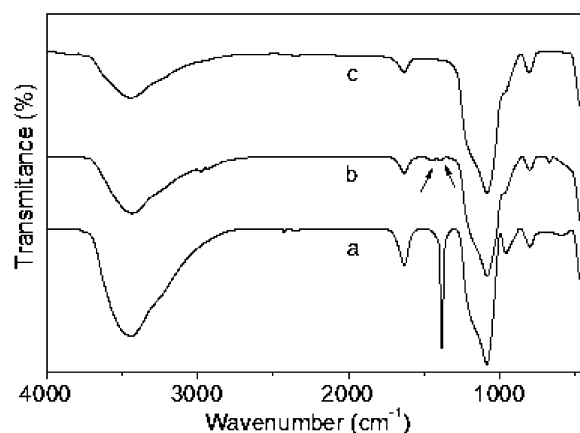

Fig. 10. IR spectra of mixCuO/SBA-15(10) pretreated for 6 h at (a) room temperature, (b) 573 K and (c) 773 K.

If mixCuO/SBA-15(5) sample was calcined at 573 K instead of at 773 K during preparation, NO_x was released rather smoothly in the range of 393–513 K without maximum and the total amount of NO_x increased further to 50.7 μmol/g. XPS test revealed that the mixCuO/SBA-15(5) sample calcined at 573 K had a higher Cu/Si molar ratio on the surface of SBA-15. Besides, some nitrogen species remained on the sample with molar ratio N/Cu close to 0.86, suggesting the existence of some surface nitrate species. When reduction takes place before complete decomposition of the nitrate, a nitrated copper surface may form [28], and the presence of two IR bands at ~1458 and 1380 cm^{-1} strongly proved the remnants of nitrate species on the surface (Fig. 10), which disappeared in the IR spectra of 773 K calcined sample. Although the nitrated copper surface formed on SBA-15 can enhance the adsorption and degradation of NPYR in the TPSR, they seem to exist in a special state as if there is no strong anchoring between them and the surface of support. 2 M HCl solution could remove the copper species in the 573 K calcined mixCuO/SBA-15(5) sample at room temperature, but failed in the 773 K calcined mixCuO/SBA-15(5) sample. Further investigation is desirable to explore the 573 K calcined sample, since advances in characterization will lead to a molecular-level understanding of the relationship between guest dispersion and catalytic performance, and the advances in synthetic methods lead to an increasingly precise control of the variables affecting catalyst activity and selectivity.

4. Conclusions

(1) Compared with wet impregnation, the solvent-free method prevents the competitive adsorption of solvent molecules on the surface of support, not

only saving the energy to remove the solvent but also providing a better dispersion of oxide species.

(2) Owing to the rich surface silanol groups along with the unique dual pore structure of SBA-15, copper, chromium and iron oxides can be spontaneously dispersed on SBA-15 by the solvent-free method, where some strong interactions occurred between the oxide species and the support.

(3) Cr(VI) dominates in the sample prepared by the solvent-free method, while Cr(III) is the main species in the corresponding impregnation sample.

(4) Nitrated copper surface can be formed over SBA-15 in case of lowering the calcination temperature of mixCuO/SBA-15 sample to 573 K, which alters the surface properties of SBA-15 and facilitates the absorption and degradation of volatile nitrosamines.

References

[1] Y. Xu, J.H. Zhu, L.L. Ma, A. Ji, Y.L. Wei, X.Y. Shang, Microporous Mesoporous Mater. 60 (2003) 125.
[2] J.H. Zhu, S.L. Zhou, Y. Xu, Y. Cao, Y.L. Wei, Chem. Lett. 32 (2003) 338.
[3] F. Schüth, A. Wingen, J. Sauer, Microporous Mesoporous Mater. 44–45 (2001) 465.
[4] J. Sauer, F. Marlow, B. Spliethoff, F. Schüth, Chem. Mater. 14 (2002) 217.
[5] T.D. Tilley, J. Mol. Catal. A 182–183 (2002) 17.
[6] S.-T. Wong, H.-P. Lin, Ch.-Y. Mou, Appl. Catal. A 198 (2000) 103.
[7] P. van der Voort, M. Mathieu, E.F. Vansant, S.N.R. Rao, M.G. White, J. Porous Mater. 5 (1998) 305.
[8] P. van der Voort, M. Morey, G.D. Stucky, M. Mathieu, E.F. Vansant, J. Phys. Chem. B 102 (1998) 585.
[9] J. Thoret, P.P. Man, E. Duprey, J. Fraissard, J. Chem. Soc., Faraday Trans. 94 (1998) 2867.
[10] C. Nozaki, C.G. Lugmair, A.T. Bell, T.D. Tilley, J. Am. Chem. Soc. 124 (2002) 13194.
[11] D. Zhao, J. Feng, Q. Huo, N. Melosh, G.H. Fredrickson, B. Chmelka, G.D. Stucky, Science 279 (1998) 548.
[12] C.T. Krege, M.E. Leonowicz, W.J. Roth, J.C. Vartuli, J.S. Beck, Nature 359 (1992) 710.
[13] R. Ryoo, C.H. Ko, M. Kruk, V. Antochshuk, M. Jaroniec, J. Phys. Chem. B 104 (2000) 11465.
[14] Y.-C. Xie, Y.-Q. Tang, Adv. Catal. 37 (1990) 1.
[15] W. Hammond, E. Prouzet, S.D. Mahanti, T.J. Pinnavaia, Microporous Mesoporous Mater. 7 (1999) 19.
[16] O.P. Tkachenko, K.V. Klementiev, E. Loffler, I. Ritzkopf, F. Schüth, M. Bandyopadhyay, S. Grabowski, H. Gies, V. Hagen, M. Muhler, L.H. Lu, R.A. Fischer, W. Grunert, Phys. Chem. Chem. Phys. 5 (2003) 4325.
[17] J. Sauer, F. Marlow, F. Schüth, Phys. Chem. Chem. Phys. 3 (2001) 5579.
[18] S. Bennici, A. Gervasini, N. Ravasio, F. Zaccheria, J. Phys. Chem. B 107 (2003) 5168.
[19] S.D. Yim, D.J. Koh, I.-S. Nam, Catal. Today 75 (2002) 269.
[20] B.M. Weckhuysen, R.A. Schoonheydt, Catal. Today 49 (1999) 441.
[21] A.B. Gaspar, J.L.F. Brito, L.C. Dieguez, J. Mol. Catal. A 203 (2003) 251.
[22] B. Notari, Adv. Catal. 41 (1999) 253.
[23] E. Fois, A. Gamba, G. Tabacchi, S. Coluccia, G. Martra, J. Phys. Chem. B 107 (2003) 10767.
[24] B. Tian, X. Liu, Ch. Yu, F. Gao, Q. Luo, S. Xie, B. Tu, D. Zhao, Chem. Commun. (2002) 1186.
[25] A.S. Karpov, J. Nuss, M. Jansen, P.E. Kazin, Y.D. Tretyakov, Solid State Sci. 5 (2003) 1277.
[26] G.R. Rao, H.R. Sahu, Proc. Indian Acad. Sci. (Chem. Sci.) 113 (2001) 651.
[27] Y. Xu, Z.Y. Yun, J.H. Zhu, J.H. Xu, H.D. Liu, Y.L. Wei, K.J. Hui, Chem. Commun. (2003) 1894.
[28] V. Higgs, J. Pritchard, Appl. Catal. 25 (1986) 149.